ISSN 1674-1056
http://cpb.iphy.ac.cn
http://iopscience.iop.org/cpb
中国物理 B
Chinese Physics
中国物理
Chinese Physics B

Optimized pulse for stimulated Raman adiabatic passage on noisy experimental platform

Zhi-Ling Wang(王志凌), Leiyinan Liu(刘雷轶男), and Jian Cui(崔健)
Citation: Chin. Phys. B, 2021, 30 (**8**): 080305. DOI: 10.1088/1674-1056/abfccb
Journal homepage: http://cpb.iphy.ac.cn; http://iopscience.iop.org/cpb

What follows is a list of articles you may be interested in

Interaction induced non-reciprocal three-level quantum transport

Sai Li(李赛), Tao Chen(陈涛), Jia Liu(刘佳), and Zheng-Yuan Xue(薛正远)
Chin. Phys. B, 2021, 30 (**6**): 060314. DOI: 10.1088/1674-1056/abee0c

Application of non-Hermitian Hamiltonian model in open quantum optical systems

Hong Wang(王虹), Yue Qin(秦悦), Jingxu Ma(马晶旭), Heng Shen(申恒), Ying Hu(胡颖), and Xiaojun Jia(贾晓军)
Chin. Phys. B, 2021, 30 (**5**): 050301. DOI: 10.1088/1674-1056/abda30

Single-photon scattering controlled by an imperfect cavity

Liwei Duan(段立伟), Qing-Hu Chen(陈庆虎)
Chin. Phys. B, 2020, 29 (**7**): 070301. DOI: 10.1088/1674-1056/ab90ee

Geometric phase of an open double-quantum-dot system detected by a quantum point contact

Qian Du(杜倩), Kang Lan(蓝康), Yan-Hui Zhang(张延惠), Lu-Jing Jiang(姜露静)
Chin. Phys. B, 2020, 29 (**3**): 030302. DOI: 10.1088/1674-1056/ab6963

Production and detection of ultracold Cs_2 molecules via four-photon adiabatic passage

Li Jian, Liu Yong, Cong Shu-Lin
Chin. Phys. B, 2014, 23 (**1**): 010308. DOI: 10.1088/1674-1056/23/1/010308

SPECIAL TOPIC — Quantum computation and quantum simulation

Optimized pulse for stimulated Raman adiabatic passage on noisy experimental platform*

Zhi-Ling Wang(王志凌), Leiyinan Liu(刘雷轶男), and Jian Cui(崔健)†

School of Physics, Beihang University, Beijing 100191, *China*

(Received 3 February 2021; revised manuscript received 15 April 2021; accepted manuscript online 29 April 2021)

Stimulated Raman adiabatic passage (STIRAP) is an important technique to manipulate quantum states in quantum simulation and quantum computation. The transformation fidelity is limited in reality due to experimental imperfections. After systematically calculating the influence of dissipation caused by thermal fluctuations and instantaneous decay of the intermediate state, we find optimized control pulses of Rydberg atom in optical tweezer to increase the STIRAP fidelity via optimal control method. All constraints of currently available control lasers have been taken into account. The transition error can be further depressed when control lasers with shorter rise time and accordingly proper total evolution time are applied. Finally, the robustness of the control pulses with respect to random deviations between the theoretical pulse shape and the implemented ones is also enhanced by additional rounds of optimizations based on ensemble averaged fidelity.

Keywords: STIRAP, dissipation, optimal control, Rydberg atom

PACS: 03.67.Lx, 03.67.Pp, 42.50.Dv, 03.67.–a **DOI:** 10.1088/1674-1056/abfccb

1. Introduction

Faithful manipulation of quantum states is at the heart of modern quantum technologies.[1] Coherent transformation between orthogonal qubit states is frequently used in various quantum simulation and quantum computation applications.[2,3] To realize such transformations, a straightforward approach would be employing Rabi oscillation[4] between the two quantum states. This approach is fast, but the timing has to be very precise even for single qubit. When it comes to the scenario of multiple qubits, synchronization is an additional difficulty. An alternative approach circumventing the obstacle of precise timing is based on adiabatic transformation of quantum states. One prominent example as such is the stimulated Raman adiabatic passage (STIRAP) technique,[5–8] which employs an intermediate state ($|m\rangle$) to mediate the transition between the initial state ($|0\rangle$) and the target state ($|1\rangle$). Although the lifetime of the intermediate state can be much shorter than the transition time between $|0\rangle$ and $|1\rangle$, the spontaneous decay of $|m\rangle$ is depressed by destructive quantum interference. The STIRAP method is thus robust against spontaneous decay of quantum states as well as the inaccuracy of experimental parameters. Therefore, it has been widely applied in many quantum systems.[9,10] However, like all other adiabatic-theorem-based methods, the standard STIRAP technique can be severely influenced by the inevitable decoherence effect in real experiments.

In order to fight against decoherence, shortcut approaches have been proposed to speed up the adiabatic transformation in STIRAP.[11–13] The logic underlying those shortcut-to-adiabatic approaches is that since decoherence affects the transition fidelity via accumulating over time, one can speed up the transition while applying sophisticated additional control Hamiltonians to cancel the diabatic transition. In this regard, several theoretical ideas such as invariant-based engineering,[14] transitionless quantum driving,[15] dressed state,[16,17] etc., have been proposed and implemented on quantum simulation experiments with cold atoms[18] and nitrogen-vacancy center in diamond.[17,19] However, the shortcut-to-adiabatic approaches, requiring the ability to solve the system analytically, are mainly limited to single qubit or few qubits systems. Moreover, the obtained additional controls from those approaches are sometimes less flexible to implement in real experiments.

On the other hand, in the era of quantum technology the request of precise and efficient manipulation of system state at the quantum level has stimulated the increasing effort of developing optimal control strategies to quantum systems. Optimal control has been recognized as a powerful method to further boost the development of quantum simulation. Recent years have witnessed the success of quantum optimal control transforming from pure mathematical control theory to many real-world applications on several experimental platforms with multiple qubits. Those platforms range from NMR,[20] NV centers in diamond,[21–23] trapped ions,[24,25] cold atoms[26–28] to superconducting circuits.[29]

In this paper, we apply an optimal control method to in-

*Project supported by the Natonal Natural Science Foundation of China (Grant No. 11904018). This research was supported by the high performance computing (HPC) resources at Beihang University and the college students' innovation and entrepreneurship training program.

†Corresponding author. E-mail: jiancui@buaa.edu.cn

© 2021 Chinese Physical Society and IOP Publishing Ltd

crease the STIRAP fidelity of real experiment in noisy environment. Although using optimal control to enhance the fidelity of STIRAP transition is a general topic for all experimental platforms, we showcase its performance via ultracold single atoms trapped in optical tweezers, which serve as a competitive candidate for quantum simulation and quantum computation. We focus on two dominant dissipative effects of such system, namely, the spontaneous decay of unstable states and the the pure dephasing dynamics caused by the Doppler effect at finite temperature.[30] We will apply the dressed Chopped RAndom Basis (dCRAB) optimal control method[31] to find the control shapes to realize the function of ideal STIRAP and at the same time suppress the detrimental dissipative effects in real experiments to the largest extent, such that the fidelity of STIRAP transition can be greatly improved. Apart from that, we will also test and enhance the robustness of the obtained control pulse shapes with respect to deviation of the experimentally implementations from the calculated shapes.

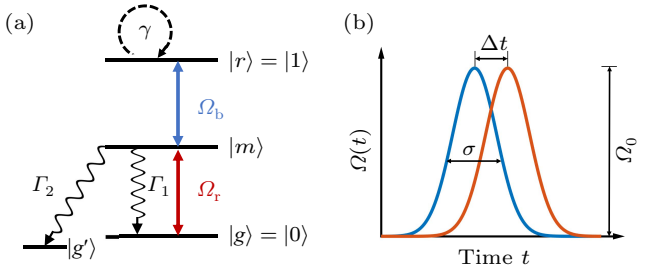


Fig. 1. Level scheme of the system. For each individual atom four relevant quantum states are involved. Qubit is defined on the ground state $|g\rangle \equiv |0\rangle$ and the excited state $|r\rangle \equiv |1\rangle$. The transition between $|0\rangle$ and $|1\rangle$ is realized through a two-photon process mediated by an intermediate state $|m\rangle$. Finally, all other states except $|g\rangle$ that the intermediate state can decay to are collectively represented as $|g'\rangle$.

2. Physical system and standard STIRAP

The physical system is arrays of single atoms trapped in optical tweezers, which can be excited to Rydberg states by external laser fields. Once such atoms are excited to Rydberg states, they will strongly interact with each other. In addition, they have relatively long coherent time and can be scaled to large qubit numbers.[32–34] Thus, they constitute a promising platform for quantum simulation. Coherent Rabi oscillation between ground state and Rydberg state has been observed in many experiments[35–39] either for single atom or multiple atoms within Rydberg blockade volume. STIRAP excitation has also been studied on such platform.[40,41] The quantum states involved in this Rydberg STIRAP scheme are shown in Fig. 1. We take a typical experimental setup reported in Refs. [30,40] as an example. The atoms are ^{87}Rb. The relevant states are the following: ground state $|g\rangle = |5S_{1/2}, F = 2, m_F = 2\rangle$, intermediate state $|m\rangle = |5P_{1/2}, F = 2, m_F = 2\rangle$, and the Rydberg state $|r\rangle = |60D_{3/2}, m_J = 3/2\rangle$. The three states forming a ladder configuration in the level scheme can be resonantly driven by the 795 nm red laser and the 475 nm blue laser, respectively. The Hamiltonian of the system with rotating wave approximation is

$$H(t) = \frac{\hbar\Omega_r(t)}{2}\sigma^x_{g,m} + \frac{\hbar\Omega_b(t)}{2}\sigma^x_{r,m}, \tag{1}$$

where $\sigma^x_{\alpha,\beta} \equiv |\alpha\rangle\langle\beta| + |\beta\rangle\langle\alpha|$. One can easily solve the single-body three-level system and obtain the eigenstates as

$$\begin{aligned} |b_+(t)\rangle &= \left(\sin\theta(t)|g\rangle + |m\rangle + \cos\theta(t)|r\rangle\right)/\sqrt{2}, \\ |b_-(t)\rangle &= \left(\sin\theta(t)|g\rangle - |m\rangle + \cos\theta(t)|r\rangle\right)/\sqrt{2}, \\ |d(t)\rangle &= \cos\theta(t)|g\rangle - \sin\theta(t)|r\rangle, \end{aligned} \tag{2}$$

where $\tan\theta(t) = \Omega_r(t)/\Omega_b(t)$. The corresponding eigenenergies are $\pm\sqrt{\Omega_b(t)^2 + \Omega_r(t)^2}/2$ and 0, respectively. Each atom is initialized in $|g\rangle$. In the ideal case, when neither dissipation occurs nor disorder exists, it is possible to transfer the atom perfectly to $|r\rangle$, if one slowly adjusts θ from 0 to π in the dark state $|d(t)\rangle$ following the adiabatic condition $\dot\theta(t) \ll \sqrt{\Omega_b(t)^2 + \Omega_r(t)^2}$. This adiabatic criterion can be satisfied by the standard STIRAP scheme, which employs two Gaussian pulses with the temporal profile

$$\Omega_{b/r}(t) = \Omega_0 \exp\left[-\frac{(t \pm \Delta t/2)^2}{2\sigma^2}\right]. \tag{3}$$

When real experimental imperfections are taken into account, however, the actual STIRAP scheme can only transfer the state with limited fidelity. In the Rydberg lattice gas system the dominant physical limitations are the Doppler dephasing effect caused by thermal fluctuations at finite temperature and the spontaneous decay from the intermediate state.[30] To simulate the dissipative dynamics under those real experimental situations we adopt the master equation in the Lindblad form

$$\dot\rho = -\mathrm{i}[H(t), \rho]/\hbar + \sum_k \left[l_k \rho l_k^\dagger - 0.5(l_k^\dagger l_k \rho + \rho l_k^\dagger l_k)\right], \tag{4}$$

where l_k represents the k-th kind dissipative jump operator. Three relevant dissipation terms are in orders. For the Doppler dephasing effect the Lindblad jump operator is $l_0 = \sqrt{\frac{\gamma}{2}}(|r\rangle\langle r| - |g\rangle\langle g|)$, where γ is the dephasing rate defined as the inverse of the pure dephasing lifetime. There are two kinds of spontaneous decays of the intermediate state, namely, the process that decays back to the ground state $|g\rangle$ used in the qubit, whose jump operator is $l_1 = \sqrt{\Gamma_1}|g\rangle\langle m|$, and those decay back to other ground states that are out of the qubit. For the latter case we label all other states in the ground states manyfold as $|g'\rangle$ and thus the jump operator is $l_2 = \sqrt{\Gamma_2}|g'\rangle\langle m|$. The parameters $\Gamma_{1,2}$ correspond to the decay rates, respectively. In this paper, we take the typical values for these dissipation rates in ongoing experiments,[30] i.e., $\gamma = 2\pi \times 120$ kHz, $\Gamma_1 = 2\Gamma/3$, $\Gamma_2 = \Gamma/3$, and $\Gamma = 2\pi \times 6$ MHz.

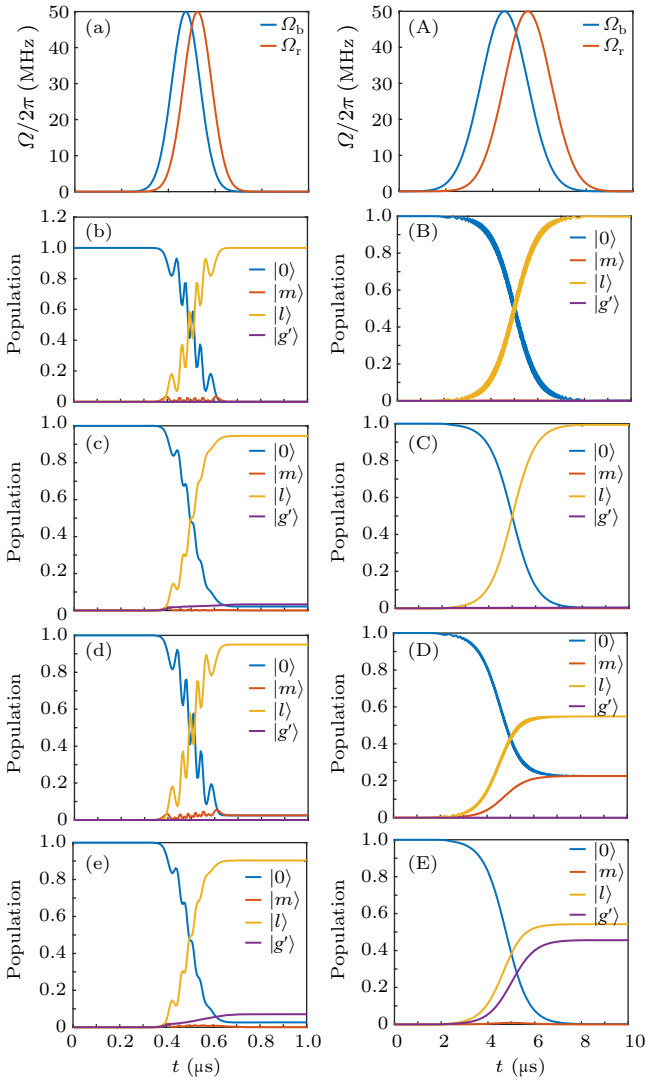


Fig. 2. Standard STIRAP for $T = 1$ μs (left) and $T = 10$ μs (right). (A, a) Pulse. Population of each state in (B, b) coherent, (C, c) only spontaneous decay, (D, d) only pure dephasing, and (E,e) both decay and dephasing dynamics.

We numerically calculate the real time dynamics of standard STIARP scheme under the decay and/or the dephasing process. In Fig. 2 we show the control pulses for the standard STIRAP and various dynamics with different total evolution time T. The left columns show the case of $T = 1$ μs, which is a typical choice in real experiment. One can see that, indeed, for the ideal case, i.e., panel (b), the STIRAP scheme works perfectly, whereas when dissipation is taken into account, the transition fidelity drops to 0.9 (panel (e)). The choice of $T = 1$ μs is made to balance the adiabatic condition and the dissipation. In order to fully expose and observe the effects of dissipation, we have calculated the case of exaggeratedly long evolution time with $T = 10$ μs and present the results in the right panels of Fig. 2. Comparing (B) and (b) it is quite obvious that the population of the intermediate state $|m\rangle$ is completely suppressed in the case of $T = 10$ μs. This explains the counterintuitive phenomenon in (C), which shows that under the decay dynamics the STIRAP scheme can reach a perfect fidelity when the total evolution time is long: from Eq. (2) one can see that the intermediate state does not appear in the dark state $|d(t)\rangle$ and therefore the spontaneous decay itself would not affect the STIRAP scheme. However, in real experiment the dephasing effect is inevitable and thus the population of the the intermediate state $|m\rangle$ is finite (panel (D)), which will trigger the spontaneous decay of the intermediate state to play its role (see panel (E)). In what follows we focus on the scenario of real experiment where both decay and dephasing coexist.

3. Optimal control method

In this paper we apply the dressed Chopped RAndom Basis (dCRAB) method,[31] optimizing the pulse shapes to increase the fidelity of STIRAP transition. We first fix the total evolution time T as well as an initial guess of the control parameter $\Omega^0(t)$, and carry out the optimization. Then optimizations with different T are performed. The dCRAB optimal control strategy iteratively updates the shape of the control pulse, which is denoted as $\Omega(t)$ in general, by multiplying $\Omega^0(t)$ with a shape function

$$g(t) \equiv 1 + \lambda(t) \sum_{k=1}^{n_c} \left[A_k^c \cos(\omega_k^c t) + A_k^s \sin(\omega_k^s t) \right], \qquad (5)$$

where $\lambda(t)$ is a filter function chosen by hand such that $\lambda(0) = \lambda(T) = 0$ and nonzero otherwise to make sure the obtained shapes always have fixed values at the initial time and the final time. The frequency $\omega_k^\alpha = (2\pi/T) \cdot B \cdot (k - 1 + r_k^\alpha)/n_c$, where $r_k^\alpha \in [0, 1]$ are constant random numbers, α takes c or s denoting the cosine or sine term, B is the bandwidth of the control parameter representing how fast the control parameter can vary over time, and n_c is the number of frequencies we keep in the modulation. One can see that the minimal possible frequency defined in this way is zero and the maximal possible value is $\omega_{max} = (2\pi/T) \cdot B$. Thus, why the bandwidth measures how fast the parameter changes is quite obvious. After taking $\Omega(t) = \Omega^0(t) \cdot g(t)$, the shape of $\Omega(t)$ is completely determined by the parameters A_k^α and then we can apply standard optimization algorithms, for instance Nelder–Mead[42] or LBFGS,[43] to iteratively optimize the shape of $\Omega(t)$ to maximize the transition fidelity $F = |\langle 1|\psi(T)\rangle|^2$. In the original CRAB method,[44,45] the random numbers r_k^α are kept constant all the way through the optimization until the stopping criteria are met. To further improve the efficiency and avoid the extrinsic local optimal traps, the original CRAB method has been upgraded to the dCRAB version,[31] which calls the original CRAB method multiple times: within each CRAB routine r_k^α remain constant, however, when the fidelity converges to a local optimal value or its increasing speed is small the CRAB routine terminates and moves on to another CRAB routine with different random r_k^α. The initial guess $\Omega^0(t)$ for the new CRAB routine is replaced by the best shape of the previous CRAB routine. The dCRAB optimization continues as such until the converged fidelity satisfies the stopping criteria.

4. Result

When applying optimal control strategies to obtain practical control schemes one has to ensure all the constraints in actual experiments be satisfied. In this paper we adopt typical constraints for ongoing Rydberg lattice gas experiments. The strength of the Rabi coupling is between zero and $2\pi \times 50$ MHz. The bandwidth of the control parameters constrains how fast one can modulate the shapes. The rise time and the fall time of the control laser are also related to the bandwidth B. We assume that the rise time is identical to the fall time, and further approximately identify them to be $t_{\rm rise} = \frac{1}{4}\frac{2\pi}{\omega_{\max}} = \frac{T}{4B}$. To obtain a set of control pulses that are experimentally easy to implement, we first chose a slow-pulse constraint, i.e., $t_{\rm rise} \geq 0.05$ μs. With this we performed the optimization with different T ranging from 0.8 μs to 1.3 μs. The best case yielded a fidelity larger than 0.98. Details can be fond in Fig. A1 in Appendix A. Compared with the standard STIRAP shown in Fig. 2(e) with approximately 0.9 fidelity, the error (measured by infidelity) has been reduced from 10% to 2%.

To further reduce the infidelity, one has to improve the current technology either reducing the dissipation rates or boosting the control. We take the second avenue. The strength of the Rabi coupling in this case reaching $2\pi \times 50$ MHz is already large enough considering the microsecond time scale. Therefore the key ingredients should be the rise time and the total duration of the control laser. Next we carried out more extensive optimizations to test how much extra gain one can expect, if the rise time of the control laser is further shortened. We decrease the rise time down to 0.01 μs and show the result in Fig. 3. For each given rise time we perform several independent optimizations with differing pulse duration T and select the best case. Note that for $t_{\rm rise} = 0.01$ μs the infidelity is shown to be 10^{-4} because lower than 10^{-4} infidelity is a sufficient condition in our stopping criteria of the optimal control.

The key advantage of STIRAP is the independence of the pulse shapes, which is of particular importance when considering real experimental implementation, where deviations from aimed pulse shapes are inevitable. Therefor, we also tested and then further enhanced the robustness of our optimized control shapes against this experimental limitation. We assume that the experimentally implemented control parameters can have random deviations from the theoretically optimized values over time. In order to evaluate the degree that the actual control shapes are different from the theoretical ones, we define the deviation rate for a given realization of the control pulses as the largest absolute deviation divide by the theoretical value. We thus generate many ensembles of random realizations with 5% deviation rate. Each ensemble has 50 members. We then further optimize the control shapes using ensemble average fidelity (The initial guess for the ensemble optimization is the optimized shape for the single shot realization, which already works fine for many members in the ensemble; after all, the realizations in the ensemble deviate from the theoretical shape only very little. Therefore, the iteration steps for the ensemble optimization to converge is not too many) as the figure of merit for the dCRAB optimization instead of the single shot fidelity. In this way, the obtained control shapes may not be the optimal ones for each individual realization, but it works commonly well for most members in the representative ensemble. We carried out this ensemble optimization based on a set of ensembles with 5% deviation rate for different rise time and then applied the ensemble optimized control shapes to an ideal realization with no deviation as well as two sets of ensembles with at most 3% and 10% deviations, respectively. The results are shown in Fig. 4. The error bar represent the worst and the best case in

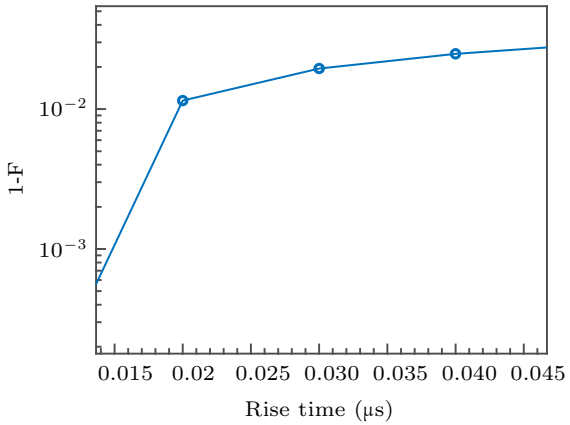


Fig. 3. Infidelity of the optimized STIRAP with different rise time. Dissipation in actual experiment is fully taken into account. The optimized control pulses for each case can be found in Fig. A1 in Appendix A.

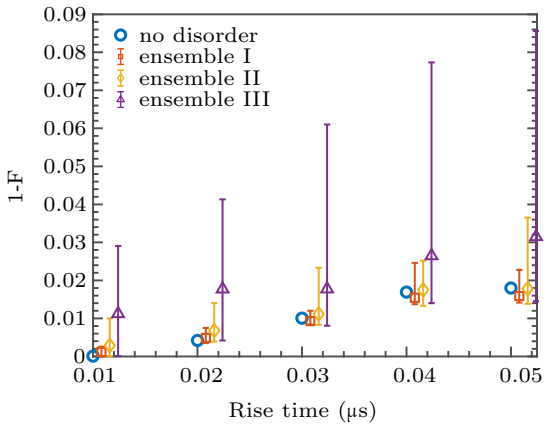


Fig. 4. Optimized STIRAP infidelity subject to different rise time in the presence of dissipation and pulse noise in terms of random deviations from the optimized control shapes. Three kinds of ensembles of disordered realizations as well as the case of no disorder are considered. Ensemble I to III correspond to the scenario of at most 3%, 5% and 10% random deviations from the optimized control shapes. Each ensemble has 50 such members. The optimizations are carried out based on the 2nd ensemble, i.e., the one with at most 5% deviations randomly occurs over time. The ensemble averages of the obtained final infidelities are shown with empty markers. The error bars represent the range of all fidelities for the realizations in the corresponding ensemble. We slightly shift the markers as well as the error bars of the disordered cases to the right in order to avoid overlaps in the plot, so that the rise time considered is respectively 0.01 μs, 0.02 μs, 0.03 μs, 0.04 μs, and 0.05 μs sharp.

each ensemble. In order for the figure to be more transparent to read, we shifted the overlape data along the horizontal direction for the ensemble averaged data. It is very clear that the deviation noise indeed has certain influence on the fidelity. However, when the deviation rate is small, the influence is negligible. In Appendix A we show the ensemble optimized control shapes as well as the dynamics in Fig. A2.

5. Discussion

In this paper we have systematically analyzed the influence of major experimental limitations on the performance of STIRAP transformation from ground state to a Rydberg excited state via an intermediate level for a single atom trapped in an optical tweezer. The limitations include the Doppler dephasing effect and spontaneous decay of the intermediate state. We then applied dCRAB optimal control strategy taking into account all relevant constraints of real experiment to obtain a set of implementable control shapes that can decrease the transition error. It is found that the transition error quantified by infidelity can be reduced from nearly 10% to 2% using the currently available control lasers. We next showed that if one continues to shorten the laser rise time and accordingly adapt the duration of the control pulse, the error can be further depressed. At last we enhanced and verified the robustness of the optimized control shapes with respect to the deviations of implemented control from the theoretical ones. Thus, the optimized control pulses are implementable and robust.

In most STIRAP experiments a detuning at the intermediate state is applied to achieve better performance. This trick can suppress the influence of instantaneous decay for the intermediate state because the detuning can reduce the possibility of occupying the unstable intermediate level to certain extent. However, we would like to find the optimal control pulses working even for the worst situations, and thus in our optimizations no detuning is applied. Our results show that even in the case of resonating controls, we manage to optimize the control pulses such that the intermediate level is almost never occupied. See the red curves in Fig. A1 representing the population of the intermediate state. It is natural to expect that if one applies detuning and carries out new optimizations, the performance of the optimized STIRAP with detuning should only be better.

In the scenario of multiple single atoms trapped in arrays of optical tweezers, which constitutes a working platform for quantum simulation, it is more difficult to perform the STIRAP transformation. The interactions between Rydberg atoms will change the dynamics, and moreover, the interaction strength depends on the intra atom distance, which will be affected by thermal fluctuations at finite temperatures. This is particularly important for the set-up employing Rydberg state, since the tweezer traps have to be switched off when applying the Rydberg lasers and thus the (thermal) motion of atoms is significant.

It is pointed out in Ref. [10] that for certain quantum simulation platforms, for instance NV centers, neither the shortcuts to adiabatic passage nor the counterdiabatic coupling scheme can effectively suppress the nonadiabatic excitation of the NV excited states to the desired level when taking into account real experimental limitations. Encouraged by the success of optimal control of STIRAP based on Rydberg atoms, it is an interesting and appealing attempt to try optimizing the STIRAP scheme on NV centers in the future.

Appendix A: Optimized control pulse shapes and the dynamics

In this appendix, we present the optimized control pulse shapes and the corresponding dynamics. the optimization is performed in two steps. First, we focus on depressing the influence of various dissipation and neglect the possibility that the experimentally implemented control pulse shape may deviate from the theoretical one. Namely, the robustness of the control pulse is not taken into account in this step. For each minimal rise time, ranging from 0.05 μs to 0.01 μs, we perform independent optimizations with various fixed total evolution time. The best case results are presented in Fig. A1.

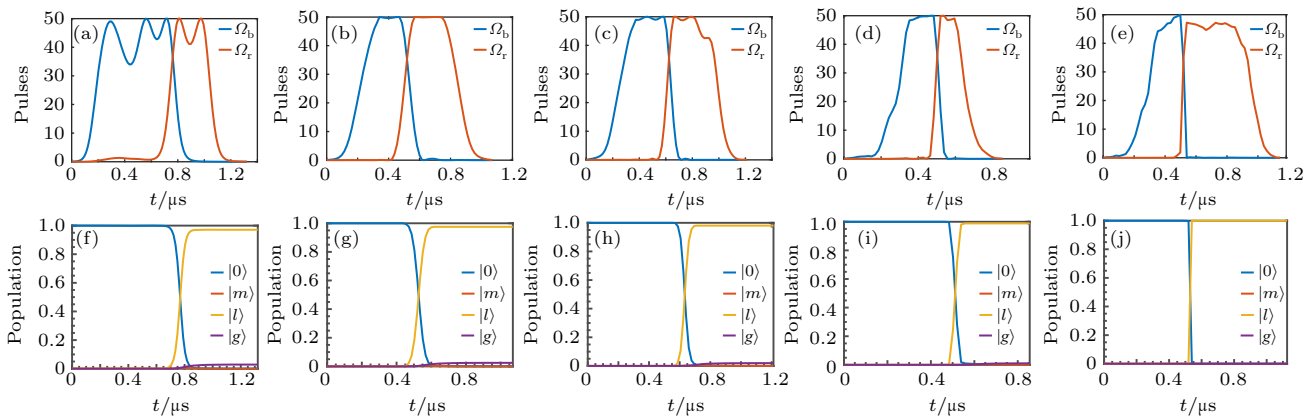


Fig. A1. The optimized STIRAP with different rise time decreasing from 0.05 μs to 0.01 μs from left to right. Top: Optimized control parameters. Bottom: Dynamics of the populations for different states. The result in Fig. 3 of the main text is obtained using the optimized pulse shapes in this figure.

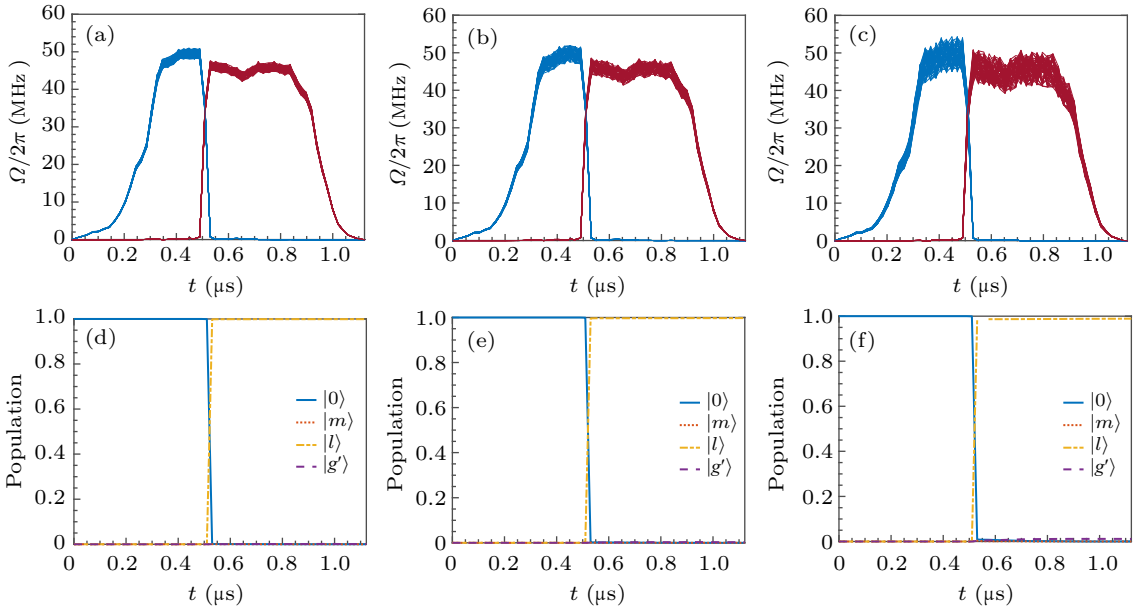


Fig. A2. The optimized STIRAP with rise time 0.01 μs. Top: Ensemble of disordered realizations of the optimized pulse shapes. Bottom: Populations of different states averaged over the ensemble. Ensemble I, II and III are arranged from left to right. The result with rise time 0.01 μs in Fig. 4 of the main text is obtained using the pulse shapes in this figure.

The second step is to enhance and verify the robustness of the optimized control shapes. To this end, we carried out the second rounds of optimizations taking the average fidelity over a sample of disordered realizations of the control pulses as the figure of merit. The previously optimized control pulse shapes are used as the input for the second optimizations. The second rounds of optimizations are performed over three independent samples with at most 3%, 5% and 10% deviations, respectively. We show the results for each sample in Fig. A2 for rise time 0.01 μs.

Acknowledgment

J.C. acknowledges helpful discussions with Thierry Lahaye, Daniel Barredo, Pascal Scholl, and Tommaso Calarco.

References

[1] Nielsen M A and Chuang I L 2011 *Quantum Computation and Quantum Information: 10th Anniversary Edition*, (Cambridge University Press)
[2] Kokail C, Maier C, van Bijnen R, Brydges T, Joshi M K, Jurcevic P, Muschik C A, Silvi P, Blatt R, Roos C F and Zoller P 2019 *Nature* **569** 355
[3] Vitanov N, Fleischhauer M, Shore B and Bergmann K 2001 *Coherent manipulation of atoms molecules by sequential laser pulses* (Academic Press) pp. 55–190
[4] Brune M 2004 *Course 3 - cavity quantum electrodynamics, in Quantum Entanglement and Information Processing*, Les Houches, Vol. 79, edited by Estève D, Raimond J M and Dalibard J (Elsevier) pp. 161–185
[5] Gaubatz U, Rudecki P, Schiemann S and Bergmann K 1990 *J. Chem. Phys.* **92** 5363
[6] Marte P, Zoller P and Hall J L 1991 *Phys. Rev. A* **44** R4118
[7] Bergmann K, Theuer H and Shore B W 1998 *Rev. Mod. Phys.* **70** 1003
[8] Vitanov N V, Rangelov A A, Shore B W and Bergmann K 2017 *Rev. Mod. Phys.* **89** 015006
[9] Bergmann K, Vitanov N V and Shore B W 2015 *J. Chem. Phys.* **142** 170901
[10] Bergmann K, Nägerl H C, Panda C, *et al.* 2019 *J. Phys. B: Atom. Mol. Opt. Phys.* **52** 202001
[11] Guéry-Odelin D, Ruschhaupt A, Kiely A, Torrontegui E, Martínez-Garaot S and Muga J G 2019 *Rev. Mod. Phys.* **91** 045001
[12] Chen X, Lizuain I, Ruschhaupt A, Guéry-Odelin D and Muga J G 2010 *Phys. Rev. Lett.* **105** 123003
[13] Ibáñez S, Chen X, Torrontegui E, Muga J G and Ruschhaupt A 2012 *Phys. Rev. Lett.* **109** 100403
[14] Chen X, Torrontegui E and Muga J G 2011 *Phys. Rev. A* **83** 062116
[15] Berry M V 2009 *J. Phys. A: Math. Theor.* **42** 365303
[16] Baksic A, Ribeiro H and Clerk A A 2016 *Phys. Rev. Lett.* **116** 230503
[17] Zhou B B, Baksic A, Ribeiro H, Yale C G, Heremans F J, Jerger P C, Auer A, Burkard G, Clerk A A and Awschalom D D 2017 *Nat. Phys.* **13** 330
[18] Du Y X, Liang Z T, Li Y C, Yue X X, Lv Q X, Huang W, Chen X, Yan H and Zhu S L 2016 *Nat. Commun.* **7** 12479
[19] Kölbl J, Barfuss A, Kasperczyk M S, Thiel L, Clerk A A, Ribeiro H and Maletinsky P 2019 *Phys. Rev. Lett.* **122** 090502
[20] Khaneja N, Reiss T, Kehlet C, Schulte-Herbrüggen T and Glaser S J 2005 *Journal of Magnetic Resonance* **172** 296
[21] Scheuer J, Kong X, Said R S, Chen J, Kurz A, Marseglia L, Du J, Hemmer P R, Montangero S, Calarco T, Naydenov B and Jelezko F 2014 *New J. Phys.* **16** 093022
[22] Dolde F, Bergholm V, Wang Y, Jakobi I, Naydenov B, Pezzagna S, Meijer J, Jelezko F, Neumann P, Schulte-Herbrüggen T, Biamonte J and Wrachtrup J 2014 *Nat. Commun.* **5** 3371
[23] Frank F, Unden T, Zoller J, Said R S, Calarco T, Montangero S, Naydenov B and Jelezko F 2017 *npj Quantum Information* **3** 48
[24] Ai M Z, Li S, Hou Z, He R, Qian Z H, Xue Z Y, Cui J M, Huang Y F, Li C F and Guo G C 2020 *Phys. Rev. Applied* **14** 054062
[25] Choi T, Debnath S, Manning T A, Figgatt C, Gong Z X, Duan L M and Monroe C 2014 *Phys. Rev. Lett.* **112** 190502
[26] Rosi S, Bernard A, Fabbri N, Fallani L, Fort C and Inguscio M 2013 *Phys. Rev. A* **88** 021601
[27] van Frank S, Bonneau M, Schmiedmayer J, Hild S, Gross C, Cheneau M, Bloch I, Pichler T, Negretti A, Calarco T and Montangero S 2016 *Sci. Rep.* **6** 34187
[28] Omran A, Levine H, Keesling A, *et al.*, 2019 *Science* **365** 570
[29] Han Z, Dong Y, Liu B, Yang X, Song S, Qiu L, Li D, Chu J, Zheng W, Xu J, Huang T, Wang Z, Yu X, Tan X, Lan D, Yung M H and Yu Y 2020 arXiv: 2004.10364 [quant-ph]
[30] de Léséleuc S, Barredo D, Lienhard V, Browaeys A and Lahaye T 2018 *Phys. Rev. A* **97** 053803
[31] Rach N, Müller M M, Calarco T and Montangero S 2015 *Phys. Rev. A* **92** 062343

[32] Endres M, Bernien H, Keesling A, Levine H, Anschuetz E R, Krajenbrink A, Senko C, Vuletic V, Greiner M and LukinMD, 2016 *Science* **54** 1024
[33] Barredo D, Léséleuc S d, Lienhard V, Lahaye T and Browaeys A 2016 *Science* **354** 1021
[34] Barredo D, Lienhard V, de Léséleuc S, Lahaye T and Browaeys A 2018 *Nature* **561** 79
[35] Miroshnychenko Y, Gaëtan A, Evellin C, Grangier P, Comparat D, Pillet P, Wilk T and Browaeys A 2010 *Phys. Rev. A* **82** 013405
[36] Reetz-Lamour M, Deiglmayr J, Amthor T and Weidemüller M 2008 *New J. Physics* **10** 045026
[37] Johnson T A, Urban E, Henage T, Isenhower L, Yavuz D D, Walker T G and Saffman M 2008 *Phys. Rev. Lett.* **100** 113003
[38] Gaëtan A, Miroshnychenko Y, Wilk T, Chotia A, Viteau M, Comparat D, Pillet P, Browaeys A and Grangier P 2009 *Nat. Phys.* **5** 115
[39] Urban E, Johnson T A, Henage T, Isenhower L, Yavuz D D, Walker T G and Saffman M 2009 *Nat. Phys.* **5** 110
[40] de Léséleuc S 2018 *Quantum simulation of spin models with assembled arrays of Rydberg atoms* (Ph.D. thesis)
[41] Gujarati T P 2018 *Phys. Rev. A* **98** 062326
[42] Press W H, Teukolsky S A, Vetterling W T and Flannery B P 2007 *Numerical Recipes*, 3rd ed. (Cambridge University Press)
[43] Coppola A and Stewart B M 2014 *lbfgs: Efficient l-bfgs and owl-qn optimization in r* (2014), software
[44] Doria P, Calarco T and Montangero S 2011 *Phys. Rev. Lett.* **106** 190501
[45] Caneva T, Calarco T and Montangero S 2011 *Phys. Rev. A* **84** 022326